Inorganic Chemistry

Article

pubs.acs.org/IC

New [ONOO]-Type Amine Bis(phenolate) Ytterbium(II) and -(III) Complexes: Synthesis, Structure, and Catalysis for Highly Heteroselective Polymerization of *rac*-Lactide

Sheng Yang, Kun Nie, Yong Zhang, Mingqiang Xue, Yingming Yao, and Qi Shen*

Key Laboratory of Organic Synthesis of Jiangsu Province, College of Chemistry, Chemical Engineering and Materials Science, Dushu Lake Campus, Soochow University, Suzhou 215123, People's Republic of China

Supporting Information

ABSTRACT: Two divalent ytterbium (Yb^{II}) complexes, **1** and **2**, supported by new [ONOO]-type amine bis(phenolate) ligands $L^{a,b}$ were synthesized in good yield by an amine elimination reaction of $Yb^{II}(N(SiMe_3)_2)_2(TMEDA)$ (TMEDA = tetramethylethylenediamine) with one equivalent of the ligand precursor. X-ray structural determination showed complexes **1** and **2** both have a monomeric structure. Each adopts distorted octahedral coordination geometry around the six-coordinate Yb^{II} ion. Two new trivalent ytterbium (Yb^{III}) aryloxide complexes, **4** and **5**, bearing [ONOO]-type amine bis(phenolate) ligands L^c and L^d were prepared by double-protonation reaction of $Yb(C_5H_5)_3THF$ with one equivalent of the ligand precursor, then one equivalent of phenol. Complex **4** has a symmetric dimeric structure with a Yb_2O_2 core bridging through the oxygen atoms of the OC_6H_4-4-CH_3 groups. Complex **5** is a THF-solvated monomer. Each six-coordinated Yb^{III} ion in both complexes adopts a distorted octahedron. All the complexes synthesized together with the known Yb^{II} complex **3** were evaluated in the ring-opening polymerization (ROP) of *rac*-lactide (*rac*-LA). Complexes **1** and **4** were found to be extremely active for controlled ROP of *rac*-LA, as judged by narrow molar mass distributions (M_w/M_n: 1.07−1.16 for complex **1** and 1.07−1.10 for complex **4**) and experimental molar mass $M_{n,exp}$ values in good agreement with theoretic $M_{n,calcd}$ values calculated on a single PLA chain produced per metal center of initiator. Complex **5** is less controlled. Complexes **1**, **4**, and **5** exhibited the same high stereoselectivity to give heterotactic polylactide with a P_r (probability of racemic enchainment of monomer units) ranging from 0.97 to 0.99. Dramatic decreases in activity and stereoselectivity were found for complexes **2** (P_r = 0.82) and **3** (P_r = 0.67), indicating the framework of L in the unit of [YbL] is crucial for determining activity and stereoselectivity of either Yb^{II} or Yb^{III} complexes.

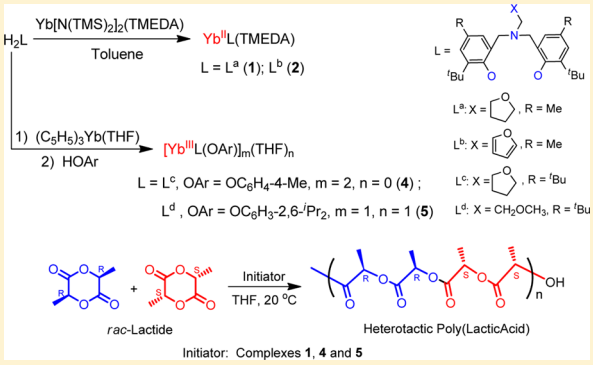

INTRODUCTION

Currently, biodegradable polymers as a promising alternative of synthetic petrochemical-based plastics have attracted considerable attention. Of the variety of biodegradable polymers known, poly(lactic acid)s (PLAs) derived from biorenewable resources have become one of the most important candidates because of their biodegradable, biocompatible nature and potential wide-ranging commercial applications (e.g., single-use packaging materials, medical sutures, and drug delivery systems).[1] Stereochemistry in PLAs plays an important role in determining the mechanical properties, biodegradability, and ultimately the end use of the material.[2] Consequently, many efforts over the past decade have been made toward the preparation of discrete, well-defined single-site catalysts for controlling the stereochemistry of lactide polymerization. A variety of systems based on metal complexes were successfully explored to prepare heterotactic and stereoblock isotactic PLA from the enantiomerically pure monomers, the racemic mixture, or *meso*-lactide.[3−10] Among the variety of initiators, trivalent lanthanide (Ln^{III}) complexes (amide, alkoxide, borohydride, and alkylide) bearing sterically demanding ancillary ligands, such as dianionic heteroatom-bridged-bisphenolate ligands, β-diiminato ligands, and salalen-type ligands, are notable as highly active for the polymerization of *rac*-LA to highly stereoselective PLAs by a chain-end control mechanism.[6−10]

Systematic studies on Ln^{III} complexes bearing various bis(phenolate) ligands have demonstrated the bridge and the ortho-phenolate substituents play a crucial role in achieving high heteroselectivity for the chain-end-controlled polymerization of *rac*-LA.[7b,6a] The Ln^{III} metal also has a great influence on the activity and selectivity.[6a,7a,10f]

Contrary to Ln^{III} complexes, the stereoselective polymerization ability of Ln^{II} complexes remains largely unexplored, although these complexes proved to be highly active initiators for ring-opening polymerization (ROP) of ε-caprolactone and L-LA as well.[11] Recently, we described the synthesis of a series

Received: July 7, 2013
Published: December 6, 2013

of Yb^{II} complexes with tetradentate bis(phenolate) ligands including amine-amine-bis(phenolate) L^e, methoxy-amine bis(phenolate) L^f, and piperazidine-bridged bis(phenolate) L^g (Figure 1) and reported for the first time the rapid, controlled,

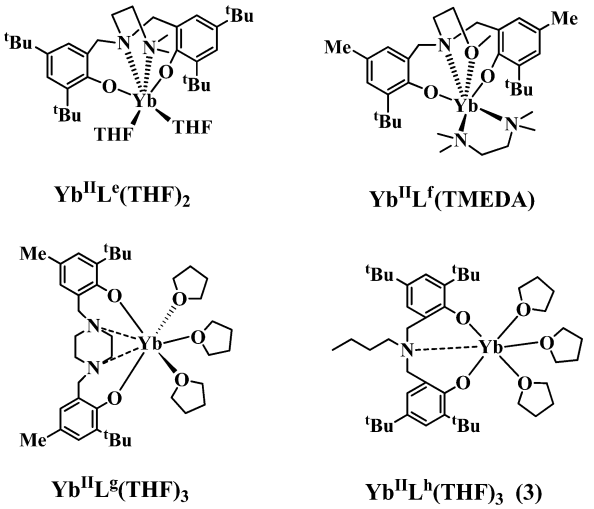

$Yb^{II}L^e(THF)_2$ $Yb^{II}L^f(TMEDA)$

$Yb^{II}L^g(THF)_3$ $Yb^{II}L^h(THF)_3$ (3)

Figure 1. Yb^{II} complexes with L^{e-g}[12] and L^h.[15]

and stereoselective ROP of *rac*-LA with complexes $Yb^{II}L^e(TMEDA)$ and $Yb^{II}L^f(TMEDA)$, forming high-heterotactic PLA with a P_r (probability of racemic enchainment of monomer units) as high as 0.99. The importance of the bridge in these ligands on the control of stereoselectivity was also demonstrated.[12] To expand upon our initial work, we were interested in investigating the effect of ligand architecture on *rac*-LA polymerization behavior of Yb^{II} complexes.

THF-amine- and furan-amine-bisphenolate ligands were first synthesized in 2003 by Moshe Kol and his co-workers. Group IV metal complexes bearing these ligands were found to be highly active 1-hexene polymerization catalysts.[13] These [ONOO]-type bis(phenolate) ligands have been used as ancillary ligands in d-block transition metal and alkaline-earth metal chemistry.[14] However, their application in designing well-defined single-site lanthanide catalysts has still remained unexplored. In this paper, we report that the new Yb^{II} complexes with [ONOO]-type bis(phenolate) ligands enable the initiation of the rapid, controlled, and stereoselective ROP of *rac*-LA, giving high-heterotactic PLAs (P_r ranging from 0.97 to 0.98). The synthesis and molecular structure of these complexes and the proposed polymerization mechanism including the real active species for the systems with Yb^{II} complexes will be presented. The synthesis and molecular structure of two new Yb^{III} aryloxide complexes with [ONOO]-bis(phenolate) ligands and their reactivity for highly heteroselective ROP of *rac*-LA are also described.

EXPERIMENTAL SECTION

General Methods. All the manipulations were performed in a pure argon atmosphere using standard Schlenk techniques or under a nitrogen atmosphere in a glovebox. The solvents were degassed and distilled from sodium benzophenone ketyl prior to use. The phenols and amines were purchased from Aldrich or Alfa Aesar. All liquids were dried over 4 Å molecular sieves for a week and distilled before use, and solid materials were used without purification. *rac*-LA (Aldrich) was recrystallized three times with dry ethyl acetate. Ligands $H_2L^{c,d}$,[13,16] $Yb^{II}(N(SiMe_3)_2)_2(TMEDA)$,[12] $Yb(C_5H_5)_3(THF)$,[17] and $Yb^{II}L^h(THF)_3$ (**3**)[15] were synthesized according to literature procedures. Rare earth metal analysis was performed by ethylenediaminetetraacetic acid titration with a xylenol orange indicator and a hexamine buffer.[18]

Instruments and Measurements. Organometallic samples for NMR spectroscopic measurements were prepared in a glovebox and then sealed by paraffin film. ^1H and ^{13}C NMR spectra were recorded on a Unity Inova-400 (FT, 400 MHz for ^1H; 100 MHz for ^{13}C) spectrometer. Homonuclear decoupled ^1H NMR spectra were recorded on a Unity Inova-400 spectrometer at 20 °C in $CDCl_3$. Carbon, hydrogen, and nitrogen analyses were performed by direct combustion with a Carlo-ErbaEA-1110 instrument. IR spectra were recorded on a Nicolet-550 Fourier transform IR spectrometer as KBr pellets. Melting points of the complexes were measured in sealed capillaries and are uncorrected. MALDI-TOF mass spectra were recorded using a Bruker Reflex II mass spectrometer (Bremen, Germany). Molar mass (M_n) and molar mass distribution (M_w/M_n) were determined against a polystyrene standard by SEC (size exclusion chromatography) on a PL 50 apparatus, and THF was used as an eluent at a flow rate of 1.0 mL min^{-1} at 40 °C. The melting point of PLA was measured at a heating rate of 2 °C on a DSC 2010TA instrument.

Synthesis of H_2L^a. A solution of 2-*tert*-butyl-4-methylphenol (16.4 g, 100 mmol), 2-(aminomethyl)tetrahydrofuran (5.21 g, 50 mmol), and 36% aqueous formaldehyde (9.7 mL, 100 mmol) in methanol (50 mL) was stirred and refluxed for 40 h. The mixture was cooled, and the supernatant solution decanted. The solid residue was triturated with ice cold methanol, filtered, and washed thoroughly with cold methanol. The ligand precursor H_2L^a was isolated as a white powder (38.5 g, 85% yield). Anal. Calcd for $C_{29}H_{43}NO_3$ (453.66): C, 76.78; H, 9.55; N, 3.09. Found: C, 76.93; H, 9.29; N, 3.25. ^1H NMR (400 MHz, C_6D_6, 25 °C): δ 8.78 (s, 2 H, ArO*H*), 6.90 (s, 2 H, Ar*H*), 6.70 (s, 2 H, Ar*H*), 4.24 (s, 1 H, C*H*O), 4.03−3.89 (m, 2 H, CH_2O), 3.73 (s, 4 H, $ArCH_2NCH_2Ar$), 2.57−2.50 (m, 2 H, NCH_2Furf), 2.23 (s, 6 H, $ArCH_3$), 1.88 (s, 4 H, CH_2CH_2), 1.39 (s, 18 H, $C(CH_3)_3$).

Synthesis of H_2L^b. A solution of 2-*tert*-butyl-4-methylphenol (8.2 g, 50 mmol), 2-(aminomethyl)furan (4.86 mL, 50 mmol), and 36% aqueous formaldehyde (9.7 mL, 100 mmol) in methanol (50 mL) was stirred and refluxed for 24 h. After cooling, another equivalent of the phenol (8.2 g, 50 mmol) was added, and the reaction was left stirring at room temperature for several days. The solvent was evaporated, and the heavy oil was left at room temperature for another two weeks, then was triturated with cold hexane, filtered, and washed thoroughly with cold hexane. The first part of H_2L^b was obtained as a white powder. The mother liquid was evaporated to give a crude oil again after a week at room temperature, and the oil was then triturated again to give more product. This procedure was repeated several times until no more solid precipitated. The total amount of product isolated in this manner was 19.3 g (43% yield). Anal. Calcd for $C_{29}H_{39}NO_3$ (449.62): C, 77.47; H, 8.74; N, 3.12. Found: C, 77.61; H, 8.39; N, 3.19. ^1H NMR (400 MHz, C_6D_6, 25 °C): δ 7.53 (s, 2 H, ArO*H*), 7.47 (s, 1 H, C*H*O), 7.01 (s, 2 H, Ar*H*), 6.76 (s, 2 H, Ar*H*), 6.38 (s, 1 H, C*H*), 6.27 (s, 1 H, C*H*), 3.67 (s, 2 H, NCH_2Furf), 3.64 (s, 4 H, $ArCH_2NCH_2Ar$), 2.24 (s, 6 H, $ArCH_3$), 1.40 (s, 18 H, $C(CH_3)_3$).

$Yb^{II}L^a(TMEDA)$ (1). A Schlenk flask was charged with H_2L^a (1.36 g, 3.00 mmol), toluene (15 mL), and a stirring bar. To this solution was added a toluene (20 mL) solution of $Yb(N(SiMe_3)_2)_2(TMEDA)$ (1.83 g, 3.00 mmol), and the color of the solution became dark green. The solution was stirred at room temperature for 12 h. After concentration, the solution was placed at −5 °C for crystallization. After several days black-red microcrystals of **1** (1.29 g, 58% based on Yb) were obtained. Mp: 154−156 °C (dec). Anal. Calcd for $YbC_{35}H_{57}N_3O_3$ (740.90): C, 56.74; H, 7.75; N, 5.67; Yb, 23.36. Found: C, 56.93; H, 7.79; N, 5.25; Yb, 23.67. ^1H NMR (400 MHz, C_6D_6, 25 °C): δ 7.01−7.36 (m, 4 H, Ar*H*), 6.90 (s, 1 H, C*H*), 4.13−4.25 (m, 2 H, CH_2O), 2.98−3.23 (m, 4 H, $ArCH_2N$), 2.62−2.69 (t, 2 H, J_{H-H} = 14 Hz, NCH_2), 2.45−2.46 (d, 6 H, J = 4 Hz, $ArCH_3$), 2.11 (s, 12 H, $N(CH_3)_2$), 1.96 (s, 4 H, CH_2CH_2), 1.74 (s, 18 H, $C(CH_3)_3$), 0.89 (s, 4 H, NCH_2CH_2N). ^{13}C NMR (100 MHz, C_6D_6, 25 °C): δ 166.11 (arom-CO), 135.65 (arom-CCH_2N), 131.58 (arom-CBu^t), 130.55 (arom-CMe), 124.47 (arom-CH), 118.08 (arom-CH), 79.56 (CH−O), 67.43 (CH_2O), 64.60

dx.doi.org/10.1021/ic401747n | *Inorg. Chem.* 2014, 53, 105−115

Table 1. Crystallographic Data for Complexes 1, 2, 4, and 5

	1	2	4	5
empirical formula	$C_{35}H_{57}N_3O_3Yb{\cdot}C_7H_8$	$C_{35}H_{53}N_3O_3Yb{\cdot}0.5C_7H_8$	$C_{84}H_{122}N_2O_8Yb_2{\cdot}C_7H_8$	$C_{49}H_{76}NO_5Yb$
fw	833.01	782.91	1726.05	932.15
temperature (K)	223(2)	223(2)	223(2)	223(2)
cryst syst	monoclinic	monoclinic	orthorhombic	orthorhombic
space group	$P2_1/c$	$P2_1/c$	$Pbcn$	$P2_12_12_1$
a (Å)	20.276(5)	13.552(4)	16.663(16)	15.387(2)
b (Å)	13.306(3)	17.092(5)	20.890(19)	16.533(2)
c (Å)	16.615(4)	17.402(6)	25.771(2)	18.915(3)
α (deg)	90	90	90	90
β (deg)	108.177(5)	104.584(7)	90	90
γ (deg)	90	90	90	90
V (Å^3)	4258.7(17)	3901(2)	8974.7(15)	4811.8(11)
Z	4	4	4	4
$D_{calcd.}$ (mg cm^{-3})	1.299	1.333	1.277	1.287
absorp coeff (mm^{-1})	2.234	2.434	2.123	1.986
$F(000)$	1728	1612	3576	1948
θ range (deg)	3.00−25.50	3.11−25.50	3.07−25.50	3.00−27.45
reflns collected/unique	20 523/7876 [R(int) = 0.0374]	18 686/7240 [R(int) = 0.0398]	36 067/8334 [R(int) = 0.0590]	22 834/10791 [R(int) = 0.0353]
data/restraints/params	7876/34/429	7240/15/408	8334/13/440	10 791/0/505
goodness-of-fit on F^2	1.086	1.142	1.157	1.077
final R [$I > 2\sigma(I)$]	0.0440	0.0548	0.0787	0.0427
wR_2 (all data)	0.1303	0.2295	0.1560	0.0843

Table 2. Selected Bond Lengths (Å) and Angles (deg) for Complexes 1 and 2

bond length	1	2	bond length	1	2
Yb(1)−N(1)	2.554(5)	2.570(6)	Yb(1)−O(1)	2.249(4)	2.188(7)
Yb(1)−N(2)	2.577(5)	2.583(8)	Yb(1)−O(2)	2.246(4)	2.239(7)
Yb(1)−N(3)	2.564(5)	2.632(10)	Yb(1)−O(3)	2.429(4)	2.656(7)
bond angle	1	2	bond angle	1	2
N(1)−Yb(1)−N(3)	168.78(15)	114.4(3)	O(1)−Yb(1)−O(3)	91.32(15)	138.9(2)
N(2)−Yb(1)−N(3)	72.82(16)	71.3(4)	O(2)−Yb(1)−O(3)	91.39(16)	87.9(2)
O(1)−Yb(1)−N(3)	103.55(16)	92.0(3)	O(1)−Yb(1)−N(1)	78.73(13)	77.6(2)
O(2)−Yb(1)−N(3)	100.01(16)	157.0(3)	O(2)−Yb(1)−N(1)	79.43(15)	79.9(2)
O(3)−Yb(1)−N(3)	99.01(15)	81.3(3)	O(3)−Yb(1)−N(1)	69.85(14)	68.7(2)
N(1)−Yb(1)−N(2)	118.34(15)	173.9(3)	O(1)−Yb(1)−N(2)	89.92(15)	100.3(3)
O(1)−Yb(1)−O(2)	155.55(15)	109.2(3)	O(2)−Yb(1)−N(2)	90.84(16)	95.6(3)
O(3)−Yb(1)−N(2)	171.79(14)	115.4(3)			

(NCH_2CHO), 56.56 ($ArCH_2N$), 54.47 (NCH_2CH_2N), 46.48 (NCH_3), 35.25 (CMe_3), 30.24 ($C(CH_3)_3$), 28.09 (THF-CH_2), 25.22 (THF-CH_2), 21.47 ($ArCH_3$). IR (KBr, cm^{-1}): 2949 (s), 2862 (s), 1631 (m), 1460 (s), 1230 (s), 1255 (s), 1035 (m), 825 (m), 632 (w), 510 (m).

$Yb^{II}L^b$(TMEDA) (2). The synthesis of complex **2** was carried out in the same way as that described for complex **1**, but Yb(N-($SiMe_3$)$_2$)$_2$(TMEDA) (1.83 g, 3.00 mmol) and H_2L^b (1.34 g, 3.00 mmol) were used. Red crystals were obtained upon crystallization from a toluene solution at room temperature (1.39 g, 63% based on Yb). Mp: 233−235 °C (dec). Anal.Calcd for $YbC_{35}H_{53}N_3O_3$ (736.87): C, 57.05; H, 7.25; N, 5.70; Yb, 23.49. Found: C, 57.40; H, 7.31; N, 5.21; Yb, 23.03. ^{1}H NMR (400 MHz, C_6D_6, 25 °C): δ 6.90−7.29 (m, 4 H, Ar*H*), 6.58 (s, 1 H, OC*H*), 5.72 (s, 1 H, CC*H*), 5.24 (s, 1 H, C*H*), 4.13−4.16 (d, 2 H, J_{H-H} = 12 Hz, $ArCH_2N$), 3.36 (s, 2 H, CCH_2), 3.08−3.11 (d, 2 H, J_{H-H} = 12 Hz, $ArCH_2N$), 2.48 (s, 6 H, $ArCH_3$), 2.11 (s, 12 H, NCH_3), 2.01 (s, 4 H, NCH_2CH_2N), 1.65 (s, 18 H, $C(CH_3)_3$). ^{13}C NMR (100 MHz, C_6D_6, 25 °C): δ 165.99 (arom-*C*O), 155.45 (*C*-O), 139.39 (*C*H−O), 135.74 (arom-*C*CH_2N), 130.83 (arom-*C*Bu^t), 129.34 (arom-*C*Me), 124.11 (arom-*C*H), 118.47 (arom-*C*H), 112.35 (*C*H), 106.68 (*C*H), 64.13 (furan-CH_2N), 57.13 ($ArCH_2N$), 46.71 (NCH_2CH_2N), 46.44 (NCH_3), 35.29 (CMe_3), 30.44 ($(CH_3)_3$), 21.43 ($ArCH_3$). IR (KBr, cm^{-1}): 2950 (s), 2846 (s), 1627 (w), 1460 (m), 1225 (s), 1160 (s), 1018 (w), 861 (w), 743 (w), 632 (m), 508 (m).

$[Yb^{III}L^c(OC_6H_4\text{-}4\text{-}CH_3)]_2$ (4). To a THF solution of Yb-(C_5H_5)$_3$(THF) (1.35 g, 3.07 mmol) was added a THF solution of H_2L^c (1.65 g, 3.07 mmol). The reaction mixture was stirred for 1 h at room temperature, and then HOC_6H_4-4-CH_3 (0.31 mL, 3.07 mmol) was added by syringe. The mixture was stirred overnight at 50 °C. The solvent was evaporated to dryness under vacuum, and toluene (10 mL) was added. The resulting solution was kept at room temperature for crystallization, and yellow crystals of complex **4** were obtained in a few days (1.75 g, 70% based on Yb). Mp: 192−194 °C (dec). Anal. Calcd for $Yb_2C_{84}H_{120}N_2O_8$ (1631.97): C, 61.82; H, 7.41; N, 1.72; Yb, 21.21. Found: C, 61.87; H, 7.39; N, 1.68; Yb, 21.18. IR (KBr, cm^{-1}): 2956 (s), 2870 (s), 1610 (m), 1506 (m), 1478 (m), 1360 (m), 1239 (s), 1156 (s), 877 (w), 835 (m), 743 (m), 639 (m), 506 (s).

$Yb^{III}L^d(OC_6H_3\text{-}2,6\text{-}{}^i\!Pr_2)$(THF) (5). The synthesis of complex **5** was carried out in the same way as that described for complex **4**, but HOC_6H_3-2,6-^{i}Pr$_2$ (0.66 mL, 3.55 mmol) was used instead of HOC_6H_4-4-CH_3. Colorless crystals of complex **5** were obtained from a toluene solution with a small amount of THF at room temperature in a few days (2.23 g, 67% based on Yb). Mp: 212−214 °C (dec). Anal. Calcd for $YbC_{49}H_{76}NO_5$ (932.15): C, 63.20; H, 8.12; N, 1.50; Yb, 18.58. Found: C, 63.23; H, 8.10; N, 1.55; Yb, 18.54. IR (KBr, cm^{-1}): 2960 (s), 2870 (s), 1602 (m), 1480 (s), 1436 (s), 1361 (m), 1234 (s), 1157 (s), 877 (w), 838 (m), 745 (m), 639 (m), 556 (m), 505 (s).

dx.doi.org/10.1021/ic401747n | Inorg. Chem. 2014, 53, 105−115

Table 3. Selected Bond Lengths (Å) and Angles (deg) for Complexes 4 and 5

bond length	4	5	bond length	4	5
Yb(1)−O(1)	2.086(6)	2.112(3)	Yb(1)−O(4)	2.279(5)	2.071(3)
Yb(1)−O(2)	2.090(6)	2.098(3)	Yb(1)−O(5)	2.253(4)	2.325(4)
Yb(1)−O(3)	2.336(6)	2.364(3)	Yb(1)−N(1)	2.434(7)	2.530(4)
bond angle	4	5	bond angle	4	5
O(1)−Yb(1)−O(2)	98.9(2)	155.51(13)	O(3)−Yb(1)−O(5)	101.62(16)	165.07(12)
O(1)−Yb(1)−O(3)	147.8(2)	93.22(14)	O(4)−Yb(1)−O(5)	71.0(2)	101.28(14)
O(1)−Yb(1)−O(4)	97.85(18)	100.40(14)	O(1)−Yb(1)−N(1)	78.5(2)	80.44(12)
O(1)−Yb(1)−O(5)	108.46(17)	85.71(13)	O(2)−Yb(1)−N(1)	81.8(2)	77.96(12)
O(2)−Yb(1)−O(3)	85.3(2)	90.00(14)	O(3)−Yb(1)−N(1)	70.5(2)	69.59(13)
O(2)−Yb(1)−O(4)	163.23(18)	103.63(14)	O(4)−Yb(1)−N(1)	102.7(2)	163.14(14)
O(2)−Yb(1)−O(5)	102.4(2)	85.02(13)	O(5)−Yb(1)−N(1)	170.95(19)	95.58(13)
O(3)−Yb(1)−O(4)	81.11(17)	93.57(13)			

Table 4. Polymerization of *rac*-LA by Complexes 1−3[a]

entry	complex	[M]/[I]	T/°C	t/h	conv (%)[b]	$M_{n,exp} \times 10^{4}$[c]	$M_{n,calcd} \times 10^{4}$[d]	M_w/M_n[c]	P_r[e]
1	**1**	400	20	1	94	6.96	5.41	1.09	0.97
2	**1**	800	20	1	79	9.85	9.10	1.09	0.99
3	**1**	800	20	2	96	10.52	11.06	1.12	0.98
4	**1**	1000	20	2	77	11.73	11.09	1.07	0.97
5	**1**	1000	20	4	90	12.18	12.96	1.16	0.98
6	**1**	2000	20	6	53	14.94	15.26	1.09	0.98
7	**1**	2000	20	12	97	27.39	27.94	1.16	0.97
8	**1**	100	60	0.4	100	1.97	1.44	1.20	0.91
9[f]	**1**	100	20	24	86	2.49	1.24	1.20	0.61
10[g]	**1**	100	20	4	83	2.83	1.20	1.15	0.90
11	**2**	100	20	24	39	2.60	0.56	1.28	0.82
12	**3**	100	20	24	26	1.51	0.37	1.38	0.67
13	$Yb^{II}L^{e}(THF)_2$[12]	800	20	2	78	8.67	8.99	1.07	0.98
14	$Yb^{II}L^{e}(THF)_2$[12]	1000	20	4	98	13.51	14.11	1.16	0.99
15	$Yb^{II}L^{f}(TMEDA)$[12]	800	20	3	100	12.45	11.52	1.09	0.97
16	$Yb^{II}L^{f}(TMEDA)$[12]	1000	20	5	96	14.00	13.82	1.10	0.97
17	$Yb^{II}L^{g}(THF)_3$[12]	100	20	1	91	2.74	1.31	1.14	0.52

[a]General polymerization conditions: solvent = THF, $[LA]_0$ = 1.0 M. [b]Conversion = weight of polymer obtained/weight of monomer used. [c]Determined by SEC against polystyrene standard and corrected by a factor of 0.58 for PLA. [d]Calculated by ([LA]/[I]) × 144.13 × X (X = conv). [e]P_r is the probability of racemic linkages between monomer units determined from the methine region of the homonuclear decoupled ^{1}H NMR spectrum. [f]Solvent = toluene. [g]Solvent = DME.

Polymerization of *rac*-LA. The polymerization proceeded in a glovebox with a 25 mL round flask. A typical polymerization procedure is as follows: To a stirred solution of *rac*-LA (0.55 g, 3.84 mmol) in 3.36 mL of THF was added a THF solution (0.48 mL) of complex **1** (0.0048 mmol, [LA] = 1.00 mol/L). The polymerization took place immediately, and the system became viscous in a few minutes at room temperature. The system kept stirring for the desired time and then was terminated by 1.0 mL of HCl/CH_3OH (0.05/10 v/v). The viscous solution was quenched by an addition of ethanol and then poured into ethanol to precipitate the polymer. The polymeric product was filtered, washed with ethanol, dried at 40 °C for 24 h in vacuo, and weighed (0.53 g, 96%).

The tacticity of the PLA was calculated according to the methine region homonuclear decoupling ^{1}H NMR spectrum. (Table 4, entry 3).

Oligomer Preparation. Oligomerization of *rac*-LA was carried out with complex **1** in THF at 25 °C at a molar ratio of [monomer]/[initiator] of 15. The reaction was stirred for 0.5 h and then quenched by adding *n*-hexane and 1 drop of water. The precipitated oligomers were collected, dried under vacuum, and used for ^{1}H NMR and MALDI-TOF mass spectra measurement.

X-ray Crystallographic Structure Determinations. Suitable single crystals of complexes **1**, **2**, **4**, and **5** were sealed in a thin-walled glass capillary for single-crystal structure determination. Intensity data were collected with a Rigaku Mercury CCD area detector in ω scan mode using Mo Kα radiation (λ = 0.71075 Å). The diffracted intensities were corrected for Lorentz/polarization effects and empirical absorption corrections. Details of the intensity data collection and crystal data are given in Table 1.

The structures were solved by direct methods and refined by full-matrix least-squares procedures based on $|F|^2$. All the non-hydrogen atoms were refined anisotropically. The hydrogen atoms in these complexes were all generated geometrically (C−H bond lengths fixed at 0.95 Å), assigned appropriate isotropic thermal parameters, and allowed to ride on their parent carbon atoms. All the H atoms were held stationary and included in the structure factor calculation in the final stage of full-matrix least-squares refinement. The structures were solved and refined by using the SHELEXL-97 program.[19] CCDC-884173 (for **1**), -884174 (for **2**), -936910 (for **4**), and -936911 (for **5**) contain the supplementary crystallographic data for this paper. These data can be obtained free of charge from The Cambridge Crystallographic Data Centre via www.ccdc.cam.ac.uk/data_request/cif.

RESULTS AND DISCUSSION

Syntheses of Complexes 1 and 2. The preligands of H_2L^a and H_2L^b were synthesized according to a reported procedure[13] as white, microcrystalline materials in moderate yields and were fully characterized.

dx.doi.org/10.1021/ic401747n | Inorg. Chem. 2014, 53, 105−115

We recently reported that the use of Yb(N-(SiMe$_3$)$_2$)$_2$(TMEDA) instead of Yb(N(SiMe$_3$)$_2$)$_2$(THF)$_2$ as a precursor in the reaction with H$_2$L^f is important for the preparation of the facile isolated complex Yb^{II}L^f(TMEDA) in high yield.[12] The same method was also used in the present case. The reaction between Yb(N(SiMe$_3$)$_2$)$_2$(THF)$_2$ and H$_2$L^a as well as H$_2$L^b led to the formation of a tar, which prevented the purification of the product. However, the title complexes were readily produced by replacing Yb(N(SiMe$_3$)$_2$)$_2$(THF)$_2$ with Yb(N(SiMe$_3$)$_2$)$_2$(TMEDA) in these reactions. Thus, the reactions of Yb(N(SiMe$_3$)$_2$)$_2$(TMEDA) with H$_2$L^{a,b} at a 1:1 molar ratio in toluene took place immediately at ambient temperature with the release of the amine HN(SiMe$_3$)$_2$. The reaction mixtures were stirred for 12 h. From the resulting solution, complexes **1** and **2** were easily isolated as red crystals in good yields (58% for complex **1**, 63% for complex **2**) (Scheme 1) upon the evaporation of volatiles and the washing of residues with hexane followed by crystallization from toluene solution.

Scheme 1. Syntheses of Complexes 1 and 2

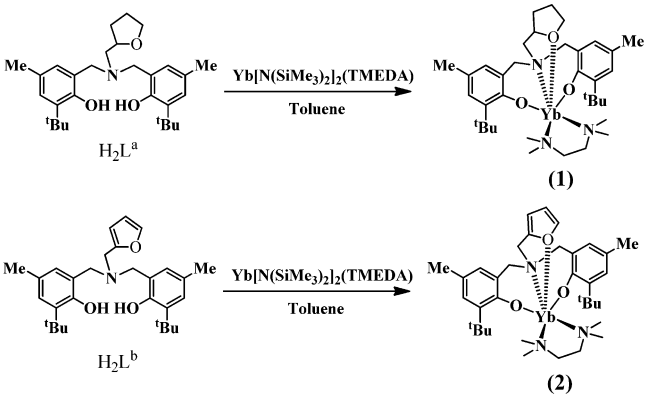

Complexes **1** and **2** have good solubility in THF and toluene and are soluble in hot hexane, but are not soluble in cold hexane. They are sensitive to air and moisture. The crystals decompose within a few minutes upon exposure to air, but the crystals and the solution are both stable when stored under argon or nitrogen. The crystals of complex **1** and complex **2** gave satisfactory elemental analyses. Their ^{1}H NMR spectra showed clear peaks that could be assigned to the ligand and the coordinated TMEDA. The identities of complexes **1** and **2** were unequivocally established by an X-ray structure determination.

Crystal Structures of Complexes 1 and 2. Crystals suitable for X-ray structural determinations of complexes **1** and **2** were obtained from a concentrated toluene solution at room temperature. Complexes **1** and **2** were crystallized as a toluene solvated **1**·toluene and a half toluene solvated **2**·0.5 toluene, respectively. The free toluene in each unit cell evaporates under vacuum, and, therefore, satisfactory elemental analysis for **1** and **2** without free toluene could be obtained (see the Experimental Section).

The molecular structures of complexes **1** and **2** are shown in Figures 2 and 3, respectively. Selected bond lengths and angles are listed in Table 2. Overall, the structures of **1** and **2** are closely related to those of the Yb^{II}L^f(TMEDA), Yb^{II}L^e(THF)$_2$,[12] and Yb^{II}L^h(THF)$_3$[15] complexes. Both complexes have a monomeric structure. Each adopts distorted octahedral coordination geometry around the ytterbium ion by

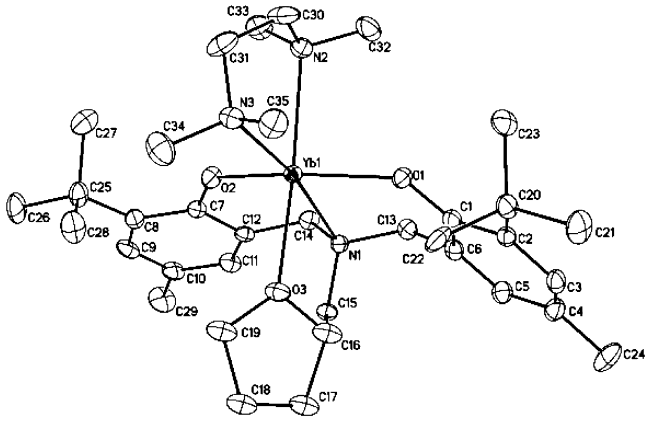

Figure 2. ORTEP diagram of the molecular structures of complex **1**. Thermal ellipsoids are drawn at the 20% probability level. All hydrogens and free solvent molecules are omitted for clarity.

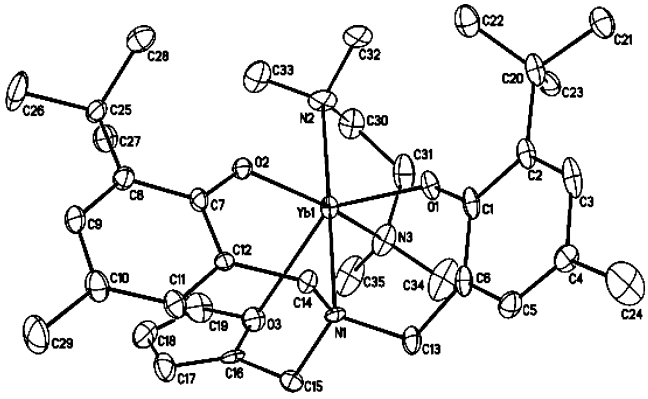

Figure 3. ORTEP diagram of the molecular structures of complex **2**. Thermal ellipsoids are drawn at the 20% probability level. All hydrogens and free solvent molecules are omitted for clarity.

one tetradentate ligand and one TMEDA molecule. In complex **1**, O(1), O(2), O(3), and N(2) occupy equatorial positions and N(1) and N(3) occupy axial positions. The N(1)−Yb−N(3) angle is slightly distorted from the ideal 180° and is 169.78(15)°. In complex **2**, O(1), O(2), O(3), and N(3) occupy equatorial positions, and N(1) and N(2) occupy axial sites with a N(1)−Yb−N(2) angle of 173.9(3)°.

The average Yb−OAr bond lengths are 2.248(4) Å (for **1**) and 2.214(7) Å (for **2**), and this is comparable with the corresponding bond lengths in the reported bridged bis-(phenolate) Yb^{II} complexes Yb^{II}L^f(TMEDA) [2.215(3) Å][12] and Yb^{II}L^e(THF)$_2$ [2.277(2) Å].[11g] These values also compare with those found in other Yb^{II} complexes containing unbridged aryloxides,[20] when the effect of the coordination number on the effective ionic radii is considered.[21] The Yb−O(ether) bond length of 2.429(4) Å in **1** is ca. 0.05 Å shorter than that found in Yb^{II}L^f(TMEDA).[12] In contrast, the Yb−O(ether) bond length (2.656(7) Å) in **2** is particularly long compared with that found for **1** and Yb^{II}L^f(TMEDA)[12] and in other Ln^{III} complexes.[6] The much longer Yb−O(ether) bond length in **2** may be attributed to a weaker side arm donor resulting in weaker binding to Yb. Such a long Yb−O(ether) bond length was also found in the zirconium complex [C$_4$H$_3$OCH$_2$N(CH$_2$-2-OC$_6$H$_2$-3,5-Bu$^t_2$)$_2$]Zr(CH$_2$Ph)$_2$ (Zr−O(ether) = 2.684(2) Å).[13]

dx.doi.org/10.1021/ic401747n | Inorg. Chem. 2014, 53, 105−115

Scheme 2. Syntheses of Complexes 4 and 5

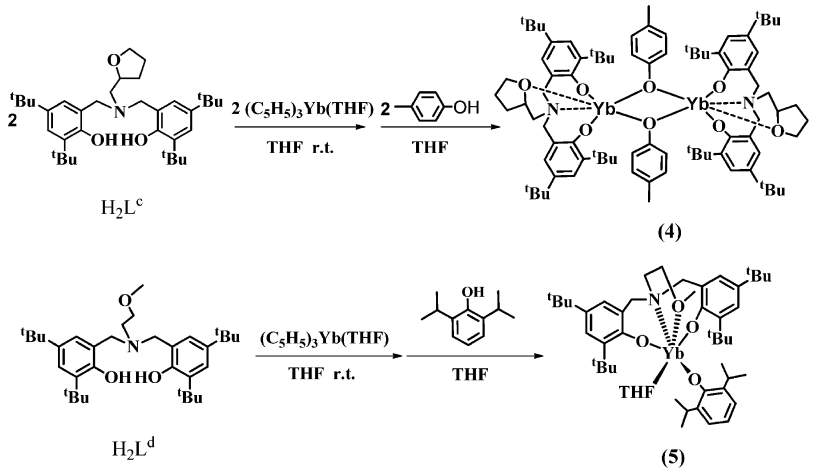

The known complex $Yb^{II}L^{h}(THF)_3$ (**3**) (Figure 1) was also prepared by amine elimination following a published procedure[15] with the aim of understanding the influence of the ligand skeleton on the catalytic behavior.

Syntheses of Complexes 4 and 5. We synthesized Yb^{III} aryloxide complexes supported by the THF-amine-bisphenolate ligand L^c and the methoxy-amine-bisphenolate ligand L^d, to compare the catalytic activity and stereoselectivity of the Yb^{II} complex with the Yb^{III} complex in the ROP of *rac*-LA. The double-protonation reaction of $Ln(C_5H_5)_3(THF)$ with an equivalent of proligand and then an equivalent of phenol was used for the syntheses of the target complexes because this procedure was recently reported to be an accessible route for the preparation of salt-free lanthanide aryloxides with a tetradentate-bridged bisphenolate ligand.[10a] The treatment of $Yb(C_5H_5)_3(THF)$ with H_2L^c in a 1:1 molar ratio in THF for 1 h and then with one equivalent of HOC_6H_4-4-CH_3 at 50 °C for another 12 h conveniently afforded the expected complex **4** as light yellow crystals in 67% yield upon crystallization from a toluene solution (Scheme 2). An attempt to synthesize isolable Yb^{III} aryloxide with ligand L^a was not successful.

The successful preparation of complex **4** led us to synthesize an analogue containing a methoxy-amine-bis(phenolate) ligand L^d,[6i] $Yb^{III}L^d(OC_6H_4$-4-$CH_3)$, using the same procedure. However, the reaction between $Yb(C_5H_5)_3(THF)$, H_2L^d, and HOC_6H_4-4-CH_3 did not afford the isolated complex in the desired yield. Fortunately, the same reaction with bulkier phenol HOC_6H_3-2,6-$^iPr_2$ proceeded smoothly, affording complex **5** as colorless crystals in 70% yield upon crystallization from a toluene solution with a small amount of THF (Scheme 2).

Complexes **4** and **5** were fully characterized, and their molecular structures were determined by single-crystal structure analysis. Both complexes are moderately sensitive to air and moisture. The crystals decompose in a few minutes when they are exposed to air, but they are thermally stable. Complexes **4** and **5** are freely soluble in THF and toluene and slightly soluble in hexane.

Crystal Structures of Complexes 4 and 5. The molecular structures of complexes **4** and **5** are shown in Figures 4 and 5, and their selective bond lengths and angles are listed in Table 3. The side arm functional group in each complex was found to bind to the metal center. Complex **4** is a symmetric dimer containing a Yb_2O_2 core bridging through the

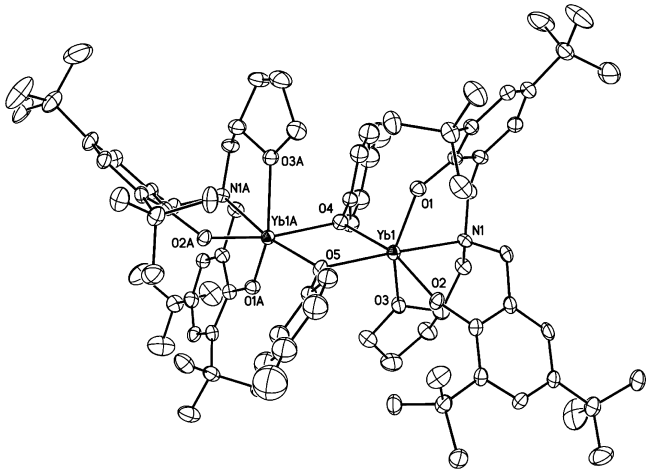

Figure 4. ORTEP diagram of the molecular structures of complex **4**. Thermal ellipsoids are drawn at the 20% probability level. All hydrogens are omitted for clarity.

oxygen atoms of the OC_6H_4-4-CH_3 groups. Each Yb^{III} atom is six-coordinate, and the coordination geometry around the Yb^{III} atom can be described as a distorted octahedron. The average bond length of Yb−O(Ar) [2.088(6) Å] is similar to that of the Ln−O(phenolate) bond.[6−10] The bond length of Yb−O(ether) is 2.336(6) Å, which is much shorter than those found in **1** and **5** and the related Ln^{III} complexes, reflecting the weak trans-influence of bridged aryloxides. The average bridged Yb−O(aryloxide) bond length of 2.266(4) Å is ca. 0.20 Å longer than the unbridged Yb−O(aryloxide) bond in **5**. This is reasonable.

Complex 5 Is a Monomer. The six-coordinated Yb^{III} ion is ligated by three oxygen atoms and one nitrogen atom from the L^d ligand, one oxygen atom from the aryloxo group, and one oxygen atom from a THF molecule in a distorted octahedron. The molecular structure of complex **5** is similar to that of the analogue $Yb^{III}L^e(OC_6H_3$-2,6-$^iPr_2)(THF)$.[10a] The average bond length of Yb−O(Ar) [2.105(3) Å] is comparable with that in complex **4**. The Yb−O(ether) bond length of 2.364(3) Å is comparable with those found in the related $YL^d[N(SiHMe_2)_2]$-(THF) and $YL^d(CH_2SiMe_3)(THF)$ complexes,[6i] if the influence of effective ionic radii is considered.[21] The Yb−O(aryloxide) bond length is normal.

dx.doi.org/10.1021/ic401747n | Inorg. Chem. 2014, 53, 105−115

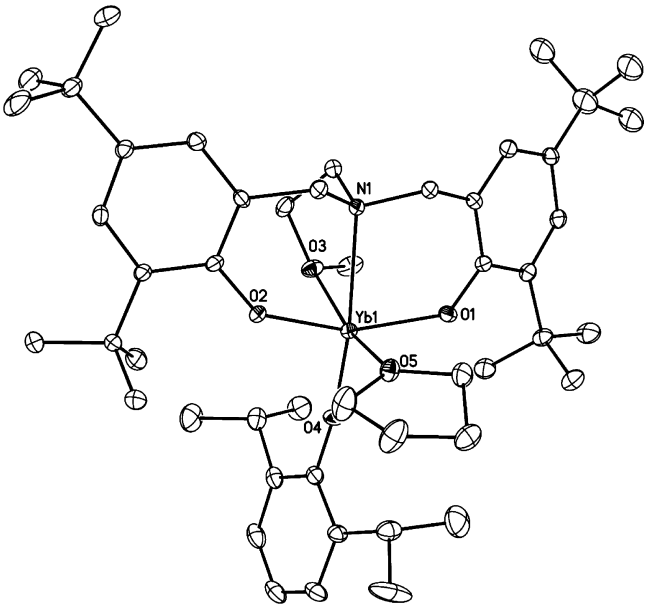

Figure 5. ORTEP diagram of the molecular structures of complex **5**. Thermal ellipsoids are drawn at the 20% probability level. All hydrogens are omitted for clarity.

ROP of *rac*-LA Initiated by Complexes 1−3. Complexes **1**−**3** were evaluated by the ROP of *rac*-LA (Scheme 3).

Scheme 3

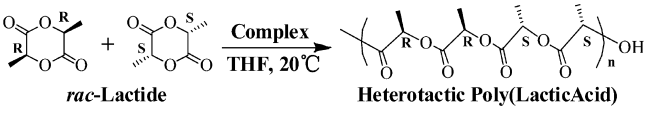

Representative results are summarized in Table 4. All complexes proved to be active initiators for the ROP of *rac*-LA under mild conditions. However, differences in activity and stereoselectivity were found. For complex **1** almost complete conversion of the monomer was achieved within 2 h at room temperature in a molar ratio of monomer to complex **1** of 800. The $M_{n,exp}$ value of the resulting PLA was very close to the $M_{n,calcd}$ value that was calculated for a single PLA chain produced per metal center of complex **1**. The molar mass distribution of the PLA was narrow (M_w/M_n =1.12, Table 4, entry 3). Complex **1** showed a high level of stereoselectivity to yield heterotactic PLA with a P_r of 0.98 (Table 4, entries 1−7). The resulting PLA has a T_m of 125 °C and no observable T_g, which is close to that reported for a heterotactic PLA.[2b] However, a significant decrease in activity and stereoselectivity was observed for complex **2** (P_r = 0.82, Table 4, entry 11). Complex **3** was even worse and showed no selectivity (P_r = 0.67, Table 4, entry 12). The catalytic behavior of complex **3** is similar to that of the reported $Yb^{II}L^g(THF)_3$ (Figure 1), as shown in Table 4, entry 17. Thus, the catalytic activity and the heterotactic selectivity of complexes **1**−**3** improved as the dative ability of the bridge increased. This significant influence of the structure of the bridge in the bisphenolate ligand on the activity and tacticity of the growing polymer chain was pointed out by Okuda's group for the ROP of *rac*-LA using Ln^{III} complexes.[7b]

The polymerization of *rac*-LA with complex **1** proceeded smoothly in monomer/**1** molar ratios ranging from 800 to 2000. The $M_{n,exp}$ values of the resulting PLAs increased proportionally with the ratio and were very close to the $M_{n,calcd}$ values that were calculated considering one polymer chain induced per metal of complex **1**. The molar mass distributions of all the PLAs remained narrow (M_w/M_n = 1.07−1.16). A slightly higher $M_{n,exp}$ (ca. 20%) than $M_{n,calcd}$ was observed when the molar ratio of monomer/**1** was lower than 800 (Table 4 entry 1). This may impact the use of polystyrene standards for SEC (size exclusion chromatography) calibration. All the obtained heterotactic PLAs had high P_r values (0.97−0.99). Moreover, the high heteroselectivity of complex **1** was not influenced by the ratio or the conversion. However, longer polymerization times and an increase in the polymerization temperature from 20 °C to 60 °C both caused some loss of heteroselectivity (Table 4, entries 7 and 8) because of transesterification side reactions. The solvent greatly influenced both the activity and stereoselectivity. THF was the optimum solvent and gave high activity and high heterotactic selectivity. The polymerization performed in DME (dimethoxyethane) at room temperature gave 83% conversion after 4 h, and the resulting PLA had a lower P_r value (P_r = 0.90, Table 4, entry 10). However, replacing THF with toluene led to a dramatic decrease in activity and heterotacticity. The polymerization became slow, and the resulting PLA was atactic (P_r = 0.61, Table 4, entry 9). The crucial role of THF in high heterotactic selectivity has been reported for Y, Zn, Ca, and well-defined Ln^{III} metal systems.[4j,k,5b,6a,9a,10f] The far higher activity in THF than in toluene is in striking contrast to the methoxy-amine-bisphenolate Ln^{III} alkoxide systems, which are able to initiate an equally rapid ROP of *rac*-LA in THF and in toluene.[6a,i] However, it is consistent with the amine-amine-bisphenolate yttrium alkyl[9a] and the 1,ω-dithiaalkanediyl-bridged bis(phenolate) Ln^{III} amide[7a] systems.

The polymerization of *rac*-LA with complex **1** has a first-order kinetic dependence on the concentration of *rac*-LA without an induction time (Figure 6), suggesting a mechanism wherein one molecule of LA per active site of catalyst is involved. The $M_{n,exp}$ values of the resulting polymers increase linearly with monomer conversion, and M_w/M_n remains within 1.09−1.10 (Figure 7). These data indicate that the polymer-

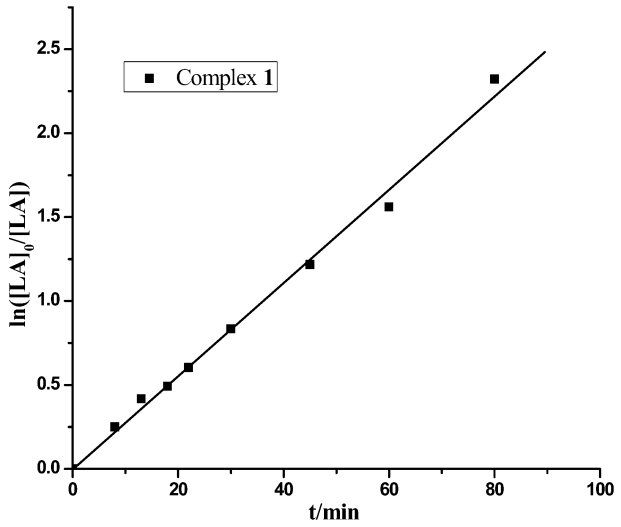

Figure 6. Plots of ln[*rac*-LA]$_0$/[*rac*-LA] vs time for ROP of *rac*-LA initiated by complex **1**. Conditions: [M]/[I] = 800, solvent = THF, [M] = 1.0 M, T = 20 °C.

dx.doi.org/10.1021/ic401747n | *Inorg. Chem.* 2014, 53, 105−115

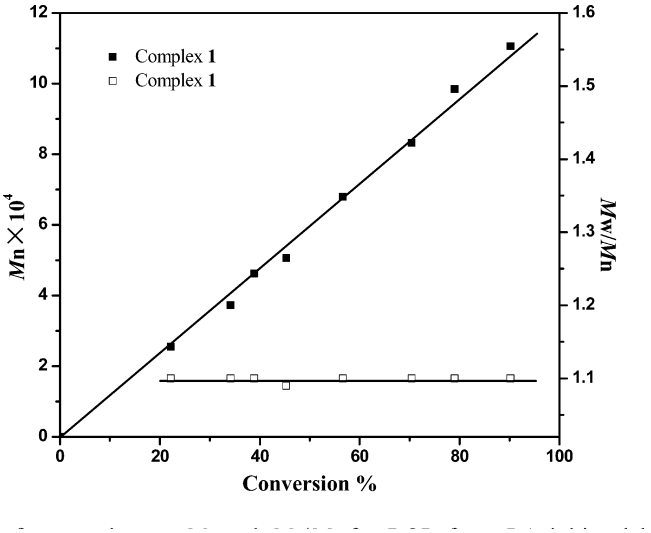

Figure 7. Plots of conversion vs M_n and M_w/M_n for ROP of *rac*-LA initiated by complex **1**. Conditions: [M]/[I] = 800, solvent = THF, [M] = 1.0 M, T = 20 °C.

ization proceeds in a living fashion, that is, without any significant side reactions. Overall, complex **1** is as good as the reported complexes $Yb^{II}L^f$(TMEDA) and $Yb^{II}L^e$(TMEDA)[12] (Figure 1) for the controlled heteroselective ROP of *rac*-LA (Table 4, entries 1−7 and 13−16).

It is presumed that the initial oxidation of a Ln^{II} complex (and concomitant monomer reduction) precedes the ROP of the cyclic ester.[11c,f] Indeed, the reaction between complex **1** and *rac*-LA in a 1:1 molar ratio yields an instant color change from deep red to pale yellow, which is indicative of Yb^{II} oxidation. Efforts to isolate and characterize the product were unsuccessful. Although the exact nature of the intermediate was not determined, a Yb^{III} species "$Yb^{III}L^aX$", where X is a ring-opened *rac*-LA, i.e., a propagating alkoxide group, is presumably formed by the oxidation of **1** with *rac*-LA. Thus, the catalytic activity of a Yb(II) complex should be related to the electron-donating ability of the ligand, which could improve the reducing ability of the Yb(II) complex. The activity sequence of **3** < **2** < **1** observed here, which is consistent with the increasing trend of the electron-donating ability of their ligands, is in accordance with the assumption.

^{1}H NMR spectroscopy of the oligomers obtained from the oligomerization of *rac*-LA with complex **1** and upon quenching with methanol and wet hexane, respectively, revealed a methoxy end group as a singlet at δ 3.74 for the former and a hydroxy group at δ 4.13 as a singlet for the latter. Obviously, the methoxy and hydroxy groups in the oligomers were derived from the corresponding quenching alcohols and water via the acylation of an electrophilic acyl end group in the original oligomer chains.[11c,12] The appearance of signals for HOC(O)-CH(CH_3) or MeOC(O)CH(CH_3) in the ^{1}H NMR spectra of the oligomers demonstrated that the PLA was linear rather than cyclic,[7c] and the polymerization proceeded by a coordination/insertion mechanism.

A MALDI-TOF mass spectrum of the oligomer was obtained upon quenching with wet hexane (Figure 8). As shown in Figure 8, the oligomer contains chains separated by lactides (144) rather than lactic acid (72) and is capped with a −OH group at one end of the chain. This indicates that almost no transesterification side reactions occurred during the lactide polymerization initiated by complex **1**. The data from the ^{1}H NMR spectrum and the MALDI-TOF mass spectrum are both in accordance with the assumption that the active species in the present polymerization system might be the "$Yb^{III}L^aX$" species (X is a ring-opened LA) that forms via the oxidation of complex **1** by *rac*-LA and the initiating group is a ring-opened LA.

ROP of *rac*-LA Initiated by Complexes 4 and 5. The proposed active species "LnLX" in the Ln^{II} complex system[11c,f] has a similar skeleton to the corresponding Ln^{III} alkoxide. Therefore, the stereocontrol of a Ln^{II} complex should be similar to that of its trivalent partner because the LnL motif around the active initiating group plays a crucial role in determining the stereocontrol of the catalyst. Indeed, the partners of $Yb^{II}L^e(THF)_2$[12] and $Yb^{III}L^e(OCH_2CF_3)(THF)$[10f] containing an amine-amine-bis(phenolate) ligand were found to have the same high heteroselectivity during the polymerization of *rac*-LA (Table 4, entry 10, and Table 5, entry 15).

Thus, complexes **4** and **5** were assessed in the ROP of *rac*-LA. The results are summarized in Table 5. Both complexes are highly stereoselective initiators, affording heterotactic PLAs with a P_r up to 0.98 in monomer/initiator molar ratios from

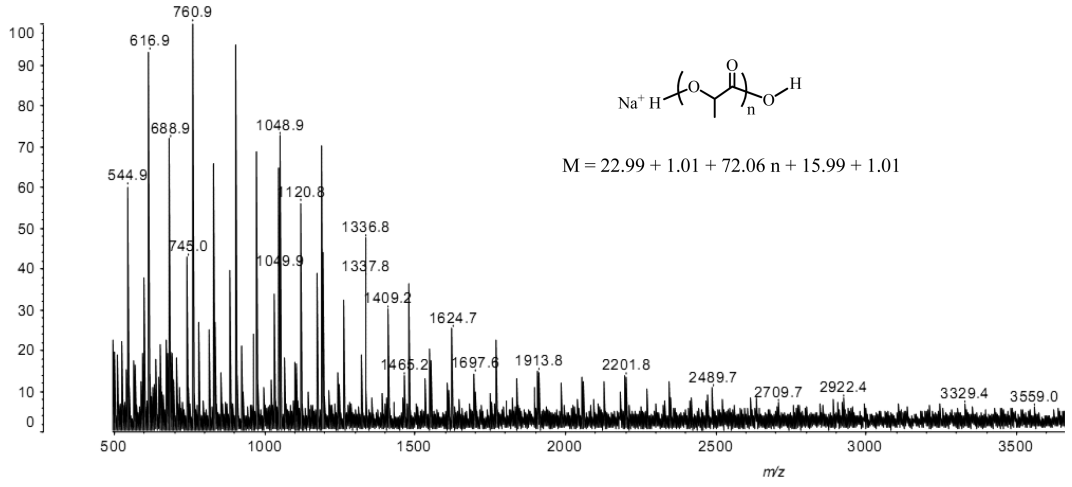

Figure 8. MALDI-TOF mass spectrum of *rac*-LA oligomer initiated by complex **1** ([M]/[I] = 20:1, in THF, 20 °C, quenching by wet hexane, doped with NaI).

dx.doi.org/10.1021/ic401747n | *Inorg. Chem.* 2014, 53, 105−115

Table 5. Polymerization of *rac*-LA by Complexes 4 and 5[a]

entry	complex	[M]/[I]	T/°C	t/min	conv (%)[b]	$M_{n,exp} \times 10^{4}$[c]	$M_{n,calcd} \times 10^{4}$[d]	M_w/M_n[c]	P_r[e]
1	**4**	400	20	30	99	6.03	5.70	1.09	0.98
2	**4**	500	20	30	99	7.08	7.13	1.09	0.98
3	**4**	600	20	30	97	7.91	8.38	1.09	0.97
4	**4**	800	20	40	98	10.96	11.29	1.07	0.97
5	**4**	1000	20	40	97	12.84	13.97	1.08	0.98
6	**4**	1200	20	40	91	13.39	15.72	1.09	0.97
7	**4**	2000	20	70	98	16.24	28.22	1.08	0.98
8	**5**	500	20	40	58	16.29	4.18	1.21	0.98
9	**5**	500	20	100	87	12.69	6.26	1.34	0.97
10	**5**	1000	20	40	52	17.15	7.49	1.19	0.98
11	**5**	2000	20	70	60	23.20	17.28	1.17	0.97
12	$YL^fN(SiHMe_2)_2$[6i]	100	20	5	100	1.55	1.44	1.33	0.80
13	$LaL^fN(SiHMe_2)_2$[6i]	100	20	5	100	2.04	1.44	1.34	0.65
14	$YL^e(OCH_2CF_3)(THF)$[10f]	1000	25	60	98	14.11	12.30	1.05	0.97
15	$Yb^{III}L^e(OCH_2CF_3)(THF)$[10f]	1000	25	60	95	13.68	16.90	1.04	0.99

[a]General polymerization conditions: solvent = THF, $[LA]_0$ = 1.0 M. [b]Conversion = weight of polymer obtained/weight of monomer used. [c]Determined by SEC against polystyrene standard and corrected by a factor of 0.58 for PLA. [d]Calculated by ([LA]/[I]) × 144.13 × X (X = conv). [e]P_r is the probability of racemic linkages between monomer units determined from the methane region of the homonuclear decoupled ^{1}H NMR spectrum.

400 to 2000 in THF at room temperature (Table 5, entries 1−11). The heteroselectivity of complexes **4** and **5** are the same as those of the corresponding divalent complexes **1** and $Yb^{II}L^f(TMEDA)$[12] (Table 4, entries 1−7, 15, and 16). This shows that the skeleton of the active species in **4** and **1**, and in **5** and $Yb^{II}L^f(TMEDA)$, is similar and the substituent at the 4-position of the phenyl ring of the tetradentate bis(phenolate) ligand has almost no influence on the stereoselectivity as pointed out before.[6a]

It is worth noting that the heterotacticity of the resulting PLA with complex **5** is much higher than those obtained by the reported analogous yttrium and lanthanum amides[6a,i] (Table 5, entries 12 and 13). This may be caused by differences in the ionic radius. An increasing sequence of La < Y < Yb was observed and is consistent with a decrease in the ionic radius of the metals. This shows the importance of the metal center in determining the stereoselectivity of a complex, as mentioned before.[12] Interestingly, replacing the $N(CH_2)_2OMe$ bridge with $N(CH_2)_2NMe_2$ did not result in a difference in stereocontrol between the analogous Y and Yb^{III} complexes (Table 5, entries 14 and 15), demonstrating that the ligand containing a $N(CH_2)_2NMe_2$ bridge is less sensitive to the metal center.

Complex **4** could act as a single-site initiator for the controlled polymerization of *rac*-LA as found for complex **1**. Polymerization systems with complex **4** gave PLAs with $M_{n,exp}$ values very close to the calculated $M_{n,calcd}$ values for a single PLA chain produced per metal center and with narrow molar mass distributions (M_w/M_n = 1.07−1.09, Table 5, entries 1−5). Complex **4** is more active than complex **1**. For example, the polymerization of *rac*-LA with complex **4** proceeded rapidly at 20 °C in THF at [*rac*-LA] = 1.0 M, resulting in the complete conversion of the monomer within 40 min in a monomer/initiator molar ratio of 1000 (Table 5, entry 5). The same polymerization with complex **1** gave 90% conversion after 4 h (Table 4, entry 5). The lower catalytic activity of **1** vs **4** may be attributed to a deactivation process from the initial redox reaction, which precedes the ring-opening polymerization of *rac*-LA.

At various monomer/initiator ratios that range from 400 to 2000, the polymerization of *rac*-LA initiated by complex **4** proceeds rapidly to give a complete conversion of the monomer within 30−70 min (time was not optimized). All the PLAs produced have narrow molar mass distributions (M_w/M_n = 1.07−1.09) and $M_{n,exp}$ values close to the $M_{n,calcd}$ values for a monomer/ytterbium ratio up to 1000 (Table 5, entries 1−5). The $M_{n,exp}$ values deviate from the $M_{n,calcd}$ values when the molar ratio of monomer to initiator increases to 1200−2000 (Table 5, entries 6 and 7). A similar phenomenon was also demonstrated by Carpentier[6b] and Coates,[3k] and this mismatch possibly arises from chain-transfer processes.

A first-order kinetic dependence on the concentration of *rac*-LA without an induction time was observed for the polymerization of *rac*-LA using complex **4** (Figure 9). The $M_{n,exp}$ values increased linearly with the conversion of the monomer and the M_w/M_n values remained in the range 1.09−1.10 (Figure 10), indicating that the polymerization proceeded in a controlled manner.

Complex **5** was found to be worse in terms of activity and controllability compared with complex **4** and its partner

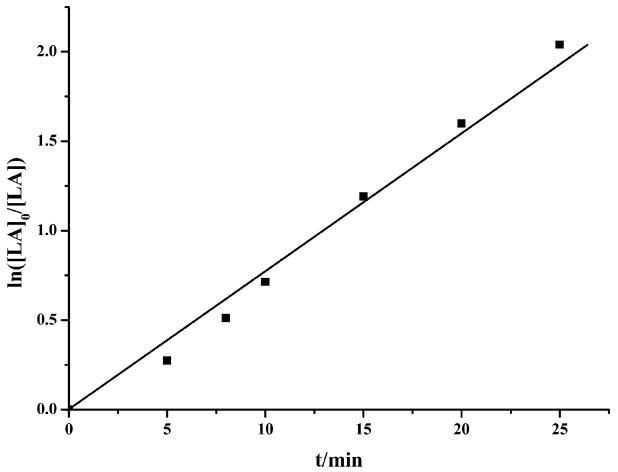

Figure 9. Plots of ln[*rac*-LA]$_0$/[*rac*-LA] vs time for ROP of *rac*-LA initiated by complex **4**. Conditions: [M]/[I] = 500, solvent = THF, [M] = 1.0 M, T = 20 °C.

dx.doi.org/10.1021/ic401747n | *Inorg. Chem.* 2014, 53, 105−115

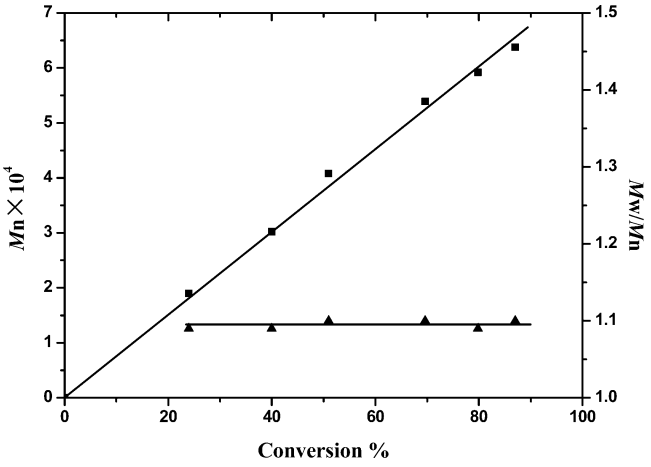

Figure 10. Plots of conversion vs M_n and M_w/M_n for ROP of *rac*-LA initiated by complex **4**. Conditions: [M]/[I] = 500, solvent = THF, [M] = 1.0 M, T = 20 °C.

$Yb^{II}L^f$(TMEDA). Polymerization with complex **5** gave 87% conversion within 100 min at a monomer/complex **5** molar ratio of 500. The resulting polymer had a far higher $M_{n,exp}$ value than the $M_{n,calcd}$ value and a broad molar mass distribution (Table 5, entry 8). This may be attributed to the much bulkier aryloxide group compared with that in complex **4**. Thus, steric crowding promoted by the aryloxide initiating group in **5** coupled with a small ytterbium ion results in a restrictive coordination environment around the Yb^{III} metal, which is less able to accommodate an incoming *rac*-LA. Therefore, the initiation efficiency of complex **5** is lower. Such a significant influence of the structure of the initiating group on activity was also found in systems containing other Ln^{III} complexes.[10a]

CONCLUSION

New Yb^{II} complexes **1** and **2** supported by THF-amine-bis(phenolate) and furan-amine-bis(phenolate), respectively, were synthesized and fully characterized. Both complexes proved to be highly heteroselective initiators, giving PLAs with a P_r up to 0.98 for **1** and 0.82 for **2**, but the known complex **3** with a amine-bis(phenolate) showed no stereoselectivity (P_r 0.67). Moreover, complex **1** enables the initiation of rapid, living polymerization of *rac*-LA, affording polymers with narrow molar mass distributions and $M_{n,exp}$ values close to $M_{n,calcd}$ values. The increasing sequence of **3** < **2** < **1** observed both for activity and heteroselectivity is consistent with the dative ability of the bridge. New Yb^{III} aryloxide complexes **4** and **5** were synthesized and structurally characterized. Complexes **4** and **5** both showed high heteroselectivity for the polymerization of *rac*-AL, giving PLAs with a P_r as high as those obtained by their divalent partners **1** and $Yb^{II}L^f$(TMEDA). This indicates that the active species in **4** (or **5**) is similar in motif to that in **1** (or $Yb^{II}L^f$(TMEDA)) and the substituent at the para-position of the phenolate ring has no influence on the stereoselectivity. A real active species "$Yb^{III}LX$", where X is a ring-opened *rac*-LA, is proposed for the present polymerizations with complexes **1**–**3** and was supported by end group analysis of oligomers using ^{1}H NMR and a MALDI-TOF mass spectrum determination.

ASSOCIATED CONTENT

Supporting Information

This material is available free of charge via the Internet at http://pubs.acs.org.

AUTHOR INFORMATION

Corresponding Author

*E-mail: qshen@suda.edu.cn. Fax: (86)512-65880305.

Notes

The authors declare no competing financial interest.

ACKNOWLEDGMENTS

We are grateful to the National Natural Science Foundation of China (Grants 20972107, 21132002, and 21372171), a project funded by the Priority Academic Program Development of Jiangsu Higher Education Institutions, for financial support.

REFERENCES

(1) (a) Drumright, R. E.; Gruber, P. R.; Henton, D. E. *Adv. Mater.* **2000**, *12*, 1841. (b) Mecking, S. *Angew. Chem., Int. Ed.* **2004**, *43*, 1078. (c) Finne, A.; Albertsson, A. C. *Biomacromolecules* **2003**, *3*, 684. (d) Kowalski, A.; Duda, A.; Penczek, S. *Macromolecules* **2000**, *33*, 689. (e) Kikkawa, Y.; Abe, H.; Iwata, T.; Inoue, Y.; Doi, Y. *Biomacromolecules* **2002**, *3*, 350. (f) Dove, A. P. *Chem. Commun.* **2008**, *48*, 6446. (g) Williams, C. K.; Hillmyer, M. A. *Polym. Rev.* **2008**, *48*, 1.

(2) (a) Dechy-Cabaret, O.; Martin-Vaca, B.; Bourissou, D. *Chem. Rev.* **2004**, *104*, 6147. (b) Stanford, M. J.; Dove, A. P. *Chem. Soc. Rev.* **2010**, *39*, 486. (c) Thomas, C. M. *Chem. Soc. Rev.* **2010**, *39*, 165. (d) Dijkstra, P. J.; Du, H.; Feijen, J. *Polym. Chem.* **2011**, *2*, 520. (e) Buffet, J. C.; Okuda, J. *Polym. Chem.* **2011**, *2*, 2758.

(3) (a) Chamberlain, B. M.; Cheng, M.; Moore, D. R.; Ovitt, T. M.; Lobkovsky, E. B.; Coates, G. W. *J. Am. Chem. Soc.* **2001**, *123*, 3229. (b) Williams, C. K.; Breyfogle, L. E.; Choi, S. K.; Nam, W.; Hillmyer, M. A.; Tolman, W. B. *J. Am. Chem. Soc.* **2003**, *125*, 11350. (c) Chen, C. T.; Chan, C. Y.; Huang, C. A.; Chen, M. T.; Peng, K. F. *Dalton Trans.* **2007**, 4073. (d) Silvernail, C. M.; Yao, L. J.; Hill, L. M. R.; Hillmyer, M. A.; Tolman, W. B. *Inorg. Chem.* **2007**, *46*, 6565. (e) Drouin, F.; Oguadinma, P. O.; Whitehorne, T. J. J.; Schaper, F. *Organometallics* **2010**, *29*, 2139. (f) Darensbourg, D. J.; Karroonnirun, O. *Inorg. Chem.* **2010**, *49*, 2360. (g) Wang, L.; Ma, H. *Dalton Trans.* **2010**, *39*, 7897. (h) Liang, L. C.; Lee, W. Y.; Tsai, T. L.; Hsua, Y. L.; Lee, T. Y. *Dalton Trans.* **2010**, *39*, 8748. (i) Petrus, R.; Sobota, P. *Organometallics* **2012**, *31*, 4755. (j) Song, S.; Zhang, X.; Ma, H.; Yang, Y. *Dalton Trans.* **2012**, *41*, 3266. (k) Rieth, L. R.; Moore, D. R.; Lobkovsky, E. B.; Coates, G. W. *J. Am. Chem. Soc.* **2002**, *124*, 15239.

(4) (a) Ovitt, T. M.; Coates, G. W. *J. Am. Chem. Soc.* **2002**, *124*, 1316. (b) Nomura, N.; Ishii, R.; Yamamoto, Y.; Kondo, T. *Chem.—Eur. J.* **2007**, *13*, 4433. (c) Bouyahyi, M.; Grunova, E.; Marquet, N.; Kirillov, E.; Thomas, C. M.; Roisnel, T.; Carpentier, J. F. *Organometallics* **2008**, *27*, 5815. (d) Pappalardo, D.; Annunziata, L.; Pellecchia, C. *Macromolecules* **2009**, *42*, 6056. (e) Nomura, N.; Akita, A.; Ishii, R.; Mizuno, M. *J. Am. Chem. Soc.* **2010**, *132*, 1750. (f) Schwarz, A. D.; Chu, Z.; Mountford, P. *Organometallics* **2010**, *29*, 1246. (g) Bouyahyi, M.; Roisnel, T.; Carpentier, J. F. *Organometallics* **2010**, *29*, 491. (h) Bakewell, C.; Platel, R. H.; Cary, S. K.; Williams, C. K. *Organometallics* **2012**, *31*, 4729. (i) Lian, B.; Ma, H.; Spaniol, T. P.; Okuda, J. *Dalton Trans.* **2009**, 9033. (j) Chisholm, M. H.; Gallucci, J. C.; Phomphrai, K. *Inorg. Chem.* **2005**, *44*, 8004. (k) Chisholm, M. H.; Gallucci, J. C.; Phomphrai, K. *Inorg. Chem.* **2004**, *43*, 6717.

(5) (a) Buffet, J. C.; Okuda, J.; Arnold, P. L. *Inorg. Chem.* **2010**, *49*, 419. (b) Chisholm, M. H.; Gallucci, J.; Phomphrai, K. *Chem. Commun.* **2003**, 48. (c) Chmura, A. J.; Davidson, M. G.; Frankis, C. J.; Jonesa, M. D.; Lunnb, M. D. *Chem. Commun.* **2008**, 1293. (d) Dove, A. P.; Gibson, V. C.; Marshall, E. L.; Rzepa, H. S.; Williams, D. J. *J. Am. Chem. Soc.* **2006**, *128*, 9834. (e) Marshall, E. L.; Gibson, V. C.; Rzepa, H. S. *J. Am. Chem. Soc.* **2005**, *127*, 6048. (f) Chmura, A. J.; Chuck, C. J.; Davidson, M. G.; Mahon, M. F. *Angew. Chem., Int. Ed.* **2007**, *46*, 2280. (g) Chmura, A. J.; Jones, M. D.; Lunn, M. D.; Wong, S. S. F. *Macromolecules* **2006**, *39*, 7250. (h) Zelikoff, A. L.; Kopilov, J.; Goldberg, I.; Kol, M. *Chem. Commun.* **2009**, 6804. (i) Stopper, A.;

Okuda, J.; Kol, M. *Macromolecules* **2012**, *45*, 698. (j) Xu, C.; Yu, I.; Mehrkhodavandi, P. *Chem. Commun.* **2012**, *48*, 6806.
(6) (a) Amgoune, A.; Thomas, C. M.; Roisnel, T.; Carpentier, J. F. *Chem.—Eur. J.* **2006**, *12*, 169. (b) Amgoune, A.; Thomas, C. M.; Ilinca, S.; Roisnel, T.; Carpentier, J. F. *Angew. Chem., Int. Ed.* **2006**, *45*, 2782. (c) Amgoune, A.; Thomas, C. M.; Carpentier, J. F. *Macromol. Rapid Commun.* **2007**, *28*, 693. (d) Bouyahyi, M.; Ajellal, N.; Kirillov, E.; Thomas, C. M.; Carpentier, J. F. *Chem.—Eur. J.* **2011**, *17*, 1872. (e) Amgoune, A.; Thomas, C. M.; Carpentier, J. F. *Pure Appl. Chem.* **2007**, *79*, 2013. (f) Ajellal, N.; Lyubov, D. M.; Sinenkov, M. A.; Fukin, G. K.; Cherkasov, A. V.; Thomas, C. M.; Carpentier, J. F.; Trifonov, A. A. *Chem.—Eur. J.* **2008**, *14*, 5440. (g) Mahrova, T. V.; Fukin, G. K.; Cherkasov, A. V.; Trifonov, A. A.; Ajellal, N.; Carpentier, J. F. *Inorg. Chem.* **2009**, *48*, 4258. (h) Grunova, E.; Kirillov, E.; Roisnel, T.; Carpentier, J. F. *Dalton Trans.* **2010**, *39*, 6739. (i) Cai, C.; Amgoune, A.; Lehmann, C. W.; Carpentier, J. F. *Chem. Commun.* **2004**, 330.
(7) (a) Ma, H.; Spaniol, T. P.; Okuda, J. *Inorg. Chem.* **2008**, *47*, 3328. (b) Ma, H.; Spaniol, T. P.; Okuda, J. *Angew. Chem., Int. Ed.* **2006**, *45*, 7818. (c) Ma, H.; Okuda, J. *Macromolecules* **2005**, *38*, 2665. (d) Buffet, J. C.; Kapelski, A.; Okuda, J. *Macromolecules* **2010**, *43*, 10201.
(8) (a) Dyer, H. E.; Huijser, S.; Schwarz, A. D.; Wang, C.; Duchateau, R.; Mountford, P. *Dalton Trans.* **2008**, 32. (b) Dyer, H. E.; Huijser, S.; Susperregui, N.; Bonnet, F.; Schwarz, A. D.; Duchateau, R.; Maron, L.; Mountford, P. *Organometallics* **2010**, *29*, 3602. (c) Clark, L.; Cushion, M. G.; Dyer, H. E.; Schwarz, A. D.; Duchateau, R.; Mountford, P. *Chem. Commun.* **2010**, *46*, 273. (d) Bonnet, F.; Cowley, A. R.; Mountford, P. *Inorg. Chem.* **2005**, *44*, 9046.
(9) (a) Liu, X.; Shang, X.; Tang, T.; Hu, N.; Pei, F.; Cui, D.; Chen, X.; Jing, X. *Organometallics* **2007**, *26*, 2747. (b) Zhao, W.; Cui, D.; Liu, X.; Chen, X. *Macromolecules* **2010**, *43*, 6678. (c) Zhao, W.; Wang, Y.; Liu, X.; Cui, D. *Chem. Commun.* **2012**, *48*, 4483.
(10) (a) Nie, K.; Gu, X.; Yao, Y.; Zhang, Y.; Shen, Q. *Dalton Trans.* **2010**, *39*, 6832. (b) Luo, Y.; Li, W.; Lin, D.; Yao, Y.; Zhang, Y.; Shen, Q. *Organometallics* **2010**, *29*, 3507. (c) Li, W.; Zhang, Z.; Yao, Y.; Zhang, Y.; Shen, Q. *Organometallics* **2012**, *31*, 3499. (d) Zhang, J.; Qiu, J.; Yao, Y.; Zhang, Y.; Shen, Q. *Organometallics* **2012**, *31*, 3138. (e) Li, W.; Xue, M.; Tu, J.; Zhang, Y.; Shen, Q. *Dalton Trans.* **2012**, *41*, 7258. (f) Nie, K.; Fang, L.; Yao, Y.; Zhang, Y.; Shen, Q.; Wang, Y. *Inorg. Chem.* **2012**, *51*, 11133. (g) Cao, T.; Buchard, A.; Goff, X. F.; Williams, C. K. *Inorg. Chem.* **2012**, *51*, 2157. (h) Otero, A.; Fernandez-Baeza, J.; Lara-Sanchez, A.; Alonso-Moreno, C.; Marquez-Segovia, I.; Sanchez-Barba, L. F.; Rodriguez, A. M. *Angew. Chem., Int. Ed.* **2009**, *48*, 2176. (i) Barba, L. F.; Hughes, D. L.; Humphrey, S. M.; Bochmann, M. *Organometallics* **2005**, *24*, 3792. (j) Bakewell, C.; Cao, T.; Long, N.; Goff, X. F. L.; Auffrant, A.; Williams, C. K. *J. Am. Chem. Soc.* **2012**, *134*, 20577. (k) Clark, L.; Deacon, G. B.; Forsyth, C. M.; Junk, P. C.; Mountford, P.; Townley, J. P. *Dalton Trans.* **2010**, *39*, 6693. (l) Clark, L.; Deacon, G. B.; Forsyth, C. M.; Junk, P. C.; Mountford, P.; Townley, J. P.; Wang, J. *Dalton Trans.* **2013**, *42*, 9294.
(11) (a) Evans, W. J.; Katsumata, H. *Macromolecules* **1994**, *27*, 2330. (b) Evans, W. J.; Katsumata, H. *Macromolecules* **1994**, *27*, 4011. (c) Nishiura, M.; Hou, Z.; Koizumi, T.-a.; Imamoto, T.; Wakatsuki, Y. *Macromolecules* **1999**, *32*, 8245. (d) Delbridge, E. E.; Dugah, D. T.; Nelson, C. R.; Skelton, B. W.; White, A. H. *Dalton Trans.* **2007**, 143. (e) Dugah, D. T.; Skelton, B. W.; Delbridge, E. E. *Dalton Trans.* **2009**, 1436. (f) Binda, P. I.; Delbridge, E. E.; Abrahamson, H. B.; Skelton, B. W. *Dalton Trans.* **2009**, 2777. (g) Zhou, H.; Guo, H.; Yao, Y.; Shen, Q. *Inorg. Chem.* **2007**, *46*, 958. (h) Deng, M.; Yao, Y.; Shen, Q.; Zhang, Y.; Sun, J. *Dalton Trans.* **2004**, 944. (i) Cui, D.; Tang, T.; Cheng, J.; Hu, N.; Cheng, W. Q.; Huang, B. T. *J. Organomet. Chem.* **2002**, *650*, 84.
(12) Yang, S.; Du, Z.; Zhang, Y.; Shen, Q. *Chem. Commun.* **2012**, *48*, 9780.
(13) Groysman, S.; Goldberg, I.; Kol, M. *Organometallics* **2003**, *22*, 3013.
(14) (a) Chowdhury, R.; Crane, A.; Fowler, C.; Kwong, P.; Kozak, C. *Chem. Commun.* **2008**, 94. (b) Safaei, E.; Wojtczak, A.; Bill, E.; Hamidi, H. *Polyhedron* **2010**, *29*, 2769. (c) Ejfler, J.; Krauzy-Dziedzic, K.; Szafert, S.; Jerzykiewicz, L.; Sobota, P. *Eur. J. Inorg. Chem.* **2010**, 3602. (d) Dean, R.; Granville, S.; Dawe, L.; Decken, A.; Hattenhauer, K.; Kozak, C. *Dalton Trans.* **2010**, *39*, 548. (e) Hasan, K.; Brown, N.; Kozak, C. *Green Chem.* **2011**, *13*, 1230. (f) Dean, R.; Fowler, C.; Hasan, K.; Kerman, K.; Kwong, P.; Trudel, S.; Leznoff, D.; Kraatz, H.; Dawe, L.; Kozak, C. *Dalton Trans.* **2012**, *41*, 4806.
(15) Guo, H.; Zhou, H.; Yao, Y.; Zhang, Y.; Shen, Q. *Dalton Trans.* **2007**, 3555.
(16) Tshuva, E. Y.; Groysman, S.; Goldberg, I.; Kol, M.; Goldschmidt, Z. *Organometallics* **2002**, *21*, 662.
(17) Birmingham, J. M.; Wilkinson, G. *J. Am. Chem. Soc.* **1956**, *78*, 42.
(18) Atwood, J.; Hunter, W.; Wayda, A.; Evans, W. *Inorg. Chem.* **1981**, *20*, 4115.
(19) Sheldrick, G. M. *SHELXL-97, Program for Crystal Structure Refinement*; Universität Göttingen: Germany, 1997.
(20) (a) van den Hende, J. R.; Hitchcock, P. B.; Holmes, S. A.; Lappert, M. F. *J. Chem. Soc., Dalton Trans.* **1995**, 1435. (b) Deacon, G.; Fanwick, P.; Gitlits, A.; Rothwell, I.; Skelton, B.; White, A. *Eur. J. Inorg. Chem.* **2001**, 1505. (c) Deacon, G.; Feng, T.; Junk, P.; Skelton, B.; White, A. *Chem. Ber.* **1997**, *130*, 851. (d) Deacon, G.; Forsyth, C.; Junk, P.; Skelton, B.; White, A. *Chem.—Eur. J.* **1999**, *5*, 1452.
(21) Shannon, R. *Acta Crystallogr., Sect. A* **1976**, *32*, 751.